Cloacaenodin, an Antimicrobial Lasso Peptide with Activity against *Enterobacter*

Drew V. Carson, Monica Patiño, Hader E. Elashal, Alexis Jaramillo Cartagena, Yi Zhang,
Megan E. Whitley, Larry So, Angelo K. Kayser-Browne, Ashlee M. Earl, Roby P. Bhattacharyya,
and A. James Link*

Read Online

ACCESS | Metrics & More | Article Recommendations | Supporting Information

ABSTRACT: Using genome mining and heterologous expression, we report the discovery and production of a new antimicrobial lasso peptide from species related to the *Enterobacter cloacae* complex. Using NMR and mass spectrometric analysis, we show that this lasso peptide, named cloacaenodin, employs a threaded lasso fold which imparts proteolytic resistance that its unthreaded counterpart lacks. Cloacaenodin has selective, low micromolar, antimicrobial activity against species related to the *E. cloacae* complex, including species implicated in nosocomial infections and against clinical isolates of carbapenem-resistant *Enterobacterales*. We further used site-directed mutagenesis to probe the importance of specific residues to the peptide's biosynthesis, stability, and bioactivity.

KEYWORDS: cloacaenodin, genome mining, antimicrobial lasso peptide, *Enterobacter cloacae*, RiPPs, carbapenem-resistant *Enterobacterales*
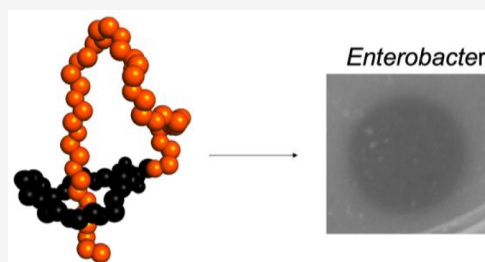
The ESKAPE pathogens are species of bacteria that are of clinical concern for their ability to evade the mechanisms of current antibiotics.[1] Without new drugs and treatments, these resistant species present a threat to humanity, causing an unnecessary loss of life to infections once treatable. The last "E" in "ESKAPE" represents species of *Enterobacter*, which is a genus of Gram-negative γ-proteobacteria.[2] While *Enterobacter* species commonly reside commensally in the human and animal GI tract and in the environment on decaying matter, in soil, and in sewage, certain species like *E. cloacae* have been the causative agents of many nosocomial outbreaks.[2–4] With the emergence of *Enterobacter* strains displaying resistance to many last-resort antibiotics like carbapenems, these concerning pathogens call for a renewed interest in development of new treatments.[3]

Within this genus is the *Enterobacter cloacae* complex (ECC) consisting of closely related species that are commonly isolated as clinical specimens, most notably *E. cloacae* and *E. hormaechei*.[4,5] Concerningly, many of these pathogens have natural resistance to β-lactam antibiotics and possess various carbapenemase genes.[3] Colistin resistance has also been increasingly found in *Enterobacter* infections.[6–12] With the rise of multidrug resistance in *Enterobacter* isolates, new compounds are sorely needed for future treatments.

A rapidly growing list of lasso peptides exhibit antimicrobial activity by several different mechanisms.[13–24] These peptides are named after their unusual threaded shape, resembling a slipknot, and are biosynthesized from a ribosomal precursor peptide (known as A) via the action of two enzymes, a protease (known as B) and lasso cyclase (known as C).[25–29] The compact, threaded structure of lasso peptides shields portions of the amide backbone, often rendering the peptides protease resistant. With advances in genomic sequencing, we can now find and predict new lasso peptides and other ribosomally synthesized and post-translationally modified peptides (RiPPs) that may not be detected from cultivation of the native species in the lab, enabling discovery of potential new drug compounds.[30–35]

Many lasso peptides display focused spectra of activity, presenting a route to target specific pathogens without disturbing commensal bacteria.[36–38] From past investigations with lasso peptides such as ubonodin,[16] citrocin,[17] klebsidin,[19] microcin J25 (MccJ25),[13] and capistruin,[14] it was noticed that these compounds often target strains that are phylogenetically similar to the producer, potentially serving as a mechanism for competition in microbial communities.[39] We thus hypothesized that lasso peptide biosynthetic gene clusters (BGCs) found in pathogen-related species would be more likely to have
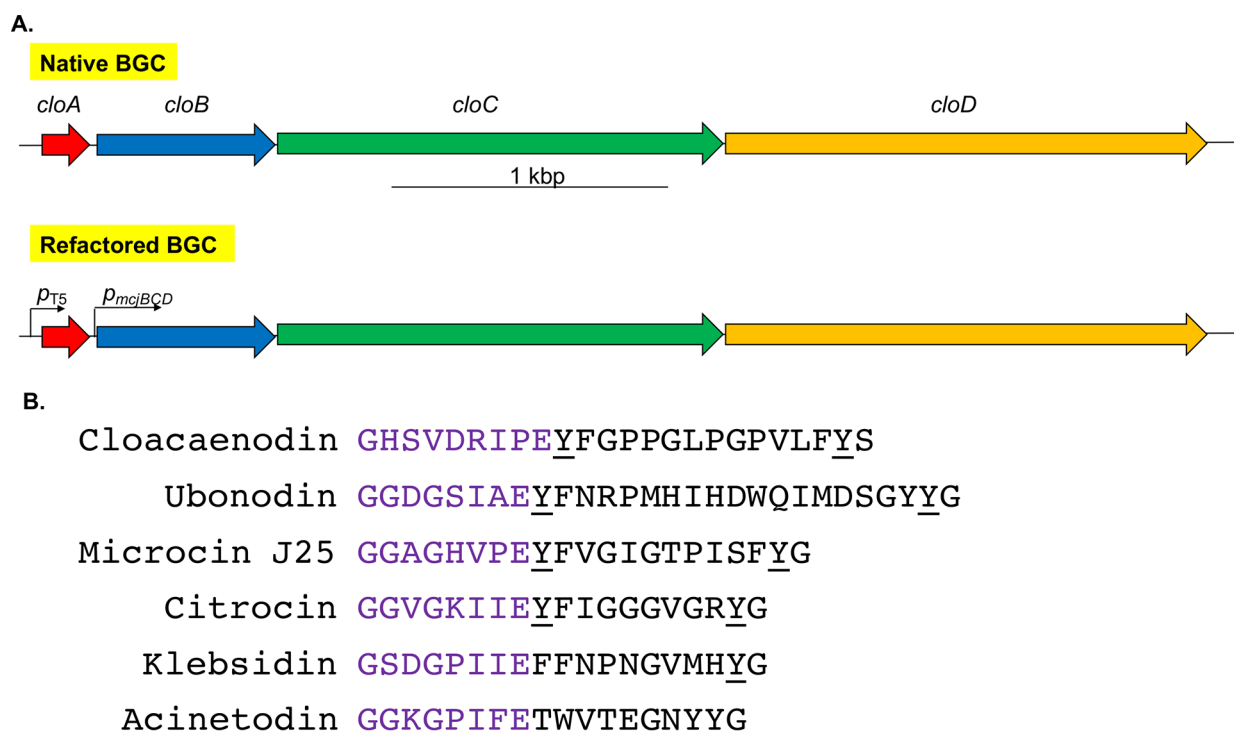
Figure 1. Genome mining reveals a new lasso peptide from *Enterobacter* species. (A) Native biosynthetic gene cluster (BGC) consists of a typical organization of lasso peptide genes in proteobacteria. It contains the precursor gene, *cloA*; the leader peptidase gene, *cloB*; the lasso peptide cyclase gene, *cloC*; and an ATP-binding cassette transporter gene for export of the mature lasso peptide, *cloD*. To facilitate heterologous expression, the BGC was codon-optimized and refactored into a pQE-80 vector with the *cloA* gene under the control of an IPTG-inducible T5 promoter, while the rest of the cluster is under the control of the constitutive p_{mcjBCD} promoter. (B) Sequence of cloacaenodin and other known RNAP-inhibiting lasso peptides. Cloacaenodin contains a 9-membered ring (purple) and a C-terminal serine, which differs from the other lasso peptides which contain an 8-membered ring and a C-terminal glycine. Cloacaenodin contains the relatively well-conserved tyrosine residue directly after the ring, and the conserved penultimate tyrosine residue (underlined).

antimicrobial activity against clinically relevant pathogens (a guilt-by-association approach), presenting an effective way to screen and prioritize genome mining hits.

Here, we report the discovery and heterologous production of a lasso peptide from members of the ECC, which we have named cloacaenodin. We solved the structure of this novel lasso peptide using solution NMR and studied its stability and structure−activity relationship via site-directed mutagenesis. Cloacaenodin showed potent and selective activity against multiple clinically relevant strains from the ECC.

■ RESULTS AND DISCUSSION

Genome Mining Reveals a New Lasso Peptide from *Enterobacter* Species. We employed our precursor-centric genome mining algorithm[26] with a particular interest in putative lasso peptides with a Tyr after the ring and a Tyr in the penultimate position. The corresponding Tyr residues in the lasso peptide MccJ25 make specific hydrogen bonding contacts in the secondary channel of RNA polymerase (RNAP).[40] We identified a putative lasso peptide BGC in *Enterobacter hormaechei* strain LB3 (on contig NZ_LFHB01000019.1), a strain that was originally identified in long beans. We later identified identical BGCs in *Enterobacter cloacae* strain B2 (on contig NZ_JSWY01000033.1), a strain isolated from bitter gourd, and *Enterobacter kobei* strain 15727[12] (on contig NZ_JAKMKX010000007.1), a strain isolated from human sputum in China. We named this lasso peptide cloacaenodin

(Figure 1), as it originates from species of the *E. cloacae* complex and the Latin root *nodum* signifies knot.

A protein BLAST search on the CloA protein revealed 14 distinct protein accession numbers corresponding to cloacaenodin-like precursors from other strains of *Salmonella*, *E. coli*, *Citrobacter*, and *Enterobacter*, including *E. cloacae* and *E. hormaechei* subsp. *xiangfangensis* (Figure S1). We queried *Enterobacter cloacae* and *Enterobacter hormaechei* in an NCBI assembly search, and found 616 total GenBank assemblies for *E. cloacae* and 3,754 total GenBank assemblies *for E. hormaechei*. Since we only observe the cloacaenodin BGC in a select few *E. cloacae* and *E. hormaechei* strains, this indicated to us that the cloacaenodin BGC is particularly rare among the currently assembled genome sequences of these two species.

From the BLAST results, we manually confirmed the presence of the *B*, *C*, and *D* genes (corresponding to the lasso peptide protease, cyclase, and exporter, respectively) downstream of the *A* gene (corresponding to the precursor). With the exception of the *E. coli* strains encoding a cloacaenodin-like precursor (Figure S1) which appear to have their *B* and *C* genes disrupted, the amino acid sequences of the biosynthetic enzymes all have at least a 50% amino acid identity to CloB, CloC, and CloD, with the D proteins having the highest degree of identity (Tables S1−S3).

Due to the producing species, this lasso peptide BGC caught our attention since we hypothesized it may have activity against members of the ECC. The gene cluster organization of *ABCD* (Figure 1A) all in a single operon is typical of proteobacterial lasso peptide gene clusters,[14] with the gene
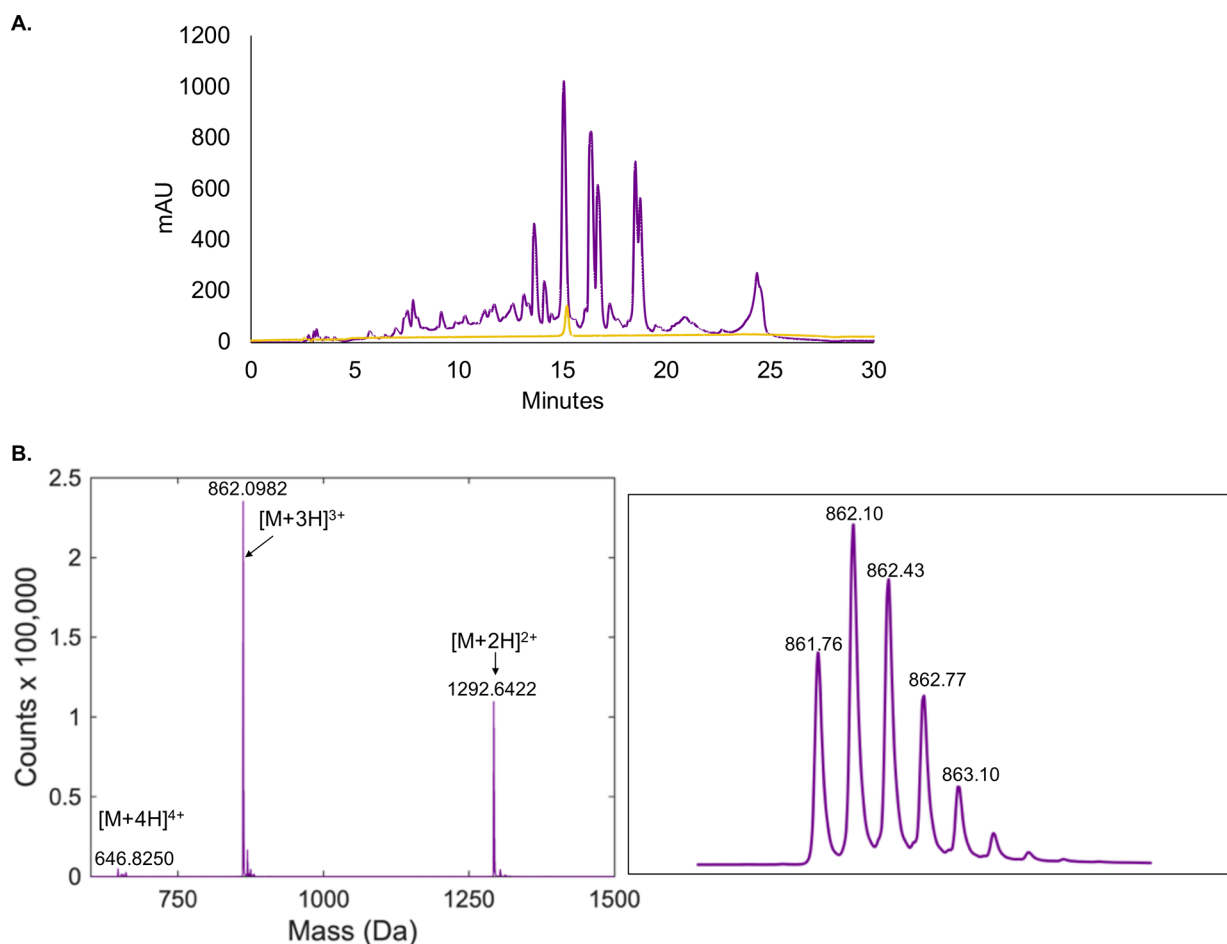
Figure 2. Cloacaenodin can be biosynthesized heterologously in *E. coli*. (A) HPLC chromatogram of the M9 supernatant extract from *E. coli* heterologous expression of cloacaenodin (purple trace) and purified cloacaenodin (light orange trace). (B) Mass spectrum of purified cloacaenodin displaying the +4, +3, and +2 charge states. A close-up of the +3 charge state isotopic distribution is shown. The expected monoisotopic +3 *m/z* is 861.77.

clusters of citrocin and MccJ25 being exceptions in which the *A* genes are transcribed divergently from the *BCD* operon.[17,41]

Our lab has previously reported the structure and activity of lasso peptides ubonodin[16] and citrocin,[17] which were shown to be potent inhibitors of RNAP, similar to the lasso peptides MccJ25, klebsidin, and acinetodin (Figure 1B).[19,40,42−44] Due to the presence of the conserved Tyr residues, we predicted that cloacaenodin may also function by inhibiting RNAP. However, the C-terminal amino acid in cloacaenodin is serine, differing from the conserved glycine seen in other RNAP-targeting lasso peptides (Figure 1B). We were thus interested to see if and how this residue would be important to the biosynthesis and activity of this new lasso peptide. Additionally, the previous RNAP-targeting lasso peptides ubonodin, citrocin, MccJ25, acinetodin, and klebsidin have been 8-membered rings, while cloacaenodin has a 9-membered ring (Figure 1B).

Heterologous Expression of Cloacaenodin. To produce the lasso peptide, we opted for a heterologous expression strategy in *E. coli*, a strategy that has historically worked well for proteobacterial lasso peptide BGCs.[45,46] We placed the *A* gene under the inducible T5 promoter in the pQE-80 plasmid with the other genes (*B*, *C*, and *D*) under the control of the constitutive p_{mcjBCD} promoter (Figure 1A). This gene refactoring strategy was originally developed for MccJ25[45]

and has been used subsequently[16,17] to allow for lasso peptide B, C, and D proteins to be already present in the cell once the A precursor is produced. To facilitate expression and eliminate any codon bias, the gene sequences were codon optimized for *E. coli*. The resulting codon-optimized BGC was synthesized as gBlocks and cloned into pQE-80. With this construct, we expressed cloacaenodin at room temperature in M9 minimal media overnight. Consistent with the presence of a *D* gene, which encodes for an ATP-binding cassette transporter that exports the lasso peptide from cells, we detected a signal that matched the expected mass of cloacaenodin in the supernatant extract through LC−MS analysis. We observed a prominent peak when extracting for the expected cloacaenodin mass and a much smaller later-eluting peak (Figure S2). Since lasso peptides are capable of unthreading,[47−49] we hypothesized that these peaks corresponded to the threaded and unthreaded variants of cloacaenodin.

We injected the supernatant extract onto an HPLC instrument and collected the prominent peak eluting at a retention time of 15.0 min (about 60/40 water/acetonitrile) (Figure 2A). Following collection, we checked this compound using LC−MS analysis, revealing a single peak that eluted at ~10.5 min, containing a species consistent with the expected mass of cloacaenodin (Figure 2B). We were able to obtain a yield of ~1.1 mg/L of culture.
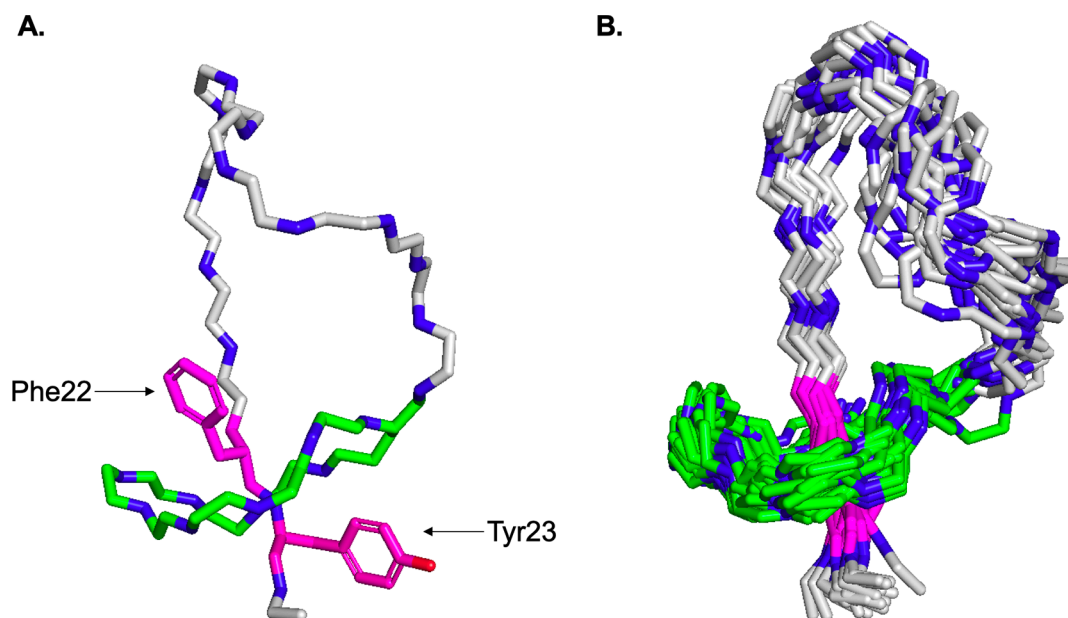
Figure 3. NMR structure of cloacaenodin. (A) Representative cloacaenodin structure is shown. Carbons from ring residues are colored in green. Carbons from loop and tail residues are colored in gray. The steric locks Phe22 and Tyr23 are displayed in magenta (oxygen for Tyr23 side chain is in red). (B) The 20 lowest energy structures are overlaid. These model structures have been deposited to the Protein Data Bank under PDB code 8DYN.

We next sought to verify the threaded nature of the collected cloacaenodin sample, as the threaded structure is crucial to the bioactivity of lasso peptides.[50] Heat treatment of certain lasso peptides leads to their irreversible unthreading; the unthreaded species often elutes differently than the threaded peptide.[48,49] We performed a heating assay at 95 °C and noticed that after 1.5 h, ~75% of cloacaenodin now eluted at around 12.4 min instead of 10.5 min (Figure S3). Upon treatment with carboxypeptidase,[48,49] this later eluting peak was eliminated, and we could then observe various earlier-eluting peaks consistent with C-terminal truncations of 6, 9, or 10 amino acids (Figures S3 and S4). We did not observe these truncations for the unheated cloacaenodin sample when treated with carboxypeptidase. This result supports our hypothesis that the smaller, and later eluting, peak in the supernatant extract is unthreaded cloacaenodin. This un-threaded variant in the extract may have formed due to thermal unthreading during expression and purification, exposure to organic solvents methanol and acetonitrile during purification, or both. To ensure that the sample we collected from the HPLC instrument remained stable, we froze the sample immediately upon collection until lyophilization, such that the peptide was minimally kept in solution.

Knowing that cloacaenodin was susceptible to unthreading, we tested how it would unthread at 37 °C, physiological temperature, in pure water. After a period of 72 h, we observed that the sample of 18 μM cloacaenodin remained ~83% threaded based on relative peak area detected via LC−MS (Figure S5). We note that it is unusual for lasso peptides to unthread at this temperature, but, in terms of bioactivity, this degree of unthreading would still provide a majority of threaded peptide to exert its function.

We performed MS/MS analysis via collision-induced dissociation (CID) on both the threaded and unthreaded conformers of cloacaenodin. We observed similar fragments for both conformers, but found that the unthreaded conformer was more prone to fragmentation than the threaded con-former, consistent with previous observations that threaded lasso peptides are resistant to fragmentation.[14,16,50] Certain fragmentation ions were only observable for the unthreaded conformer (Figure S6).

NMR Structure of Cloacaenodin. We next sought to determine the structure of cloacaenodin in water using 2D NMR analysis, a technique that has been successfully used to show the threaded shape of lasso peptides.[51] We were concerned about cloacaenodin unthreading during the NMR acquisition, which we addressed by keeping the sample at 4 °C throughout acquisition. LC−MS analysis of the sample prior to and following NMR data collection confirmed that cloacaeno-din remained threaded (Figure S7). As an additional control, 1D NMR spectra were acquired in between each 2D spectrum acquisition to ensure stability of the sample (Figure S8).

We acquired TOCSY at a mixing time of 80 ms (Figure S9) along with two NOESY spectra: one at 150 ms (Figure S10) and one at 300 ms (Figure S11). The TOCSY and 300 ms NOESY were used together to assign proton shifts (Table S8). We note that this NMR analysis was particularly challenging due to the presence of five prolines in the sequence. In addition to the prolines disrupting the NOESY walk during the assignment of residues, these prolines can lead to multiple isomers of cloacaenodin due to *cis/trans* isomerization as observed previously in MccJ25.[52] We found multiple possibilities in our assignments of Pro17 and Gly18 (Table S8), and due to this ambiguity in assigning the chemical shifts for these protons, we chose to leave these residues undefined in our model building. The chemical shifts for the amide protons of Phe22 and Tyr23 (9.210 and 10.320 ppm, respectively) are markedly downshifted from the BMRB average; the unique chemical environment experienced by these residues suggest that they may be the amino acids passing through the isopeptide bonded ring. The wide dispersion of the amide proton chemical shifts in the spectra (6.364 ppm −10.320 ppm) provides further support for the lassoed structure of cloacaenodin as it has been previously
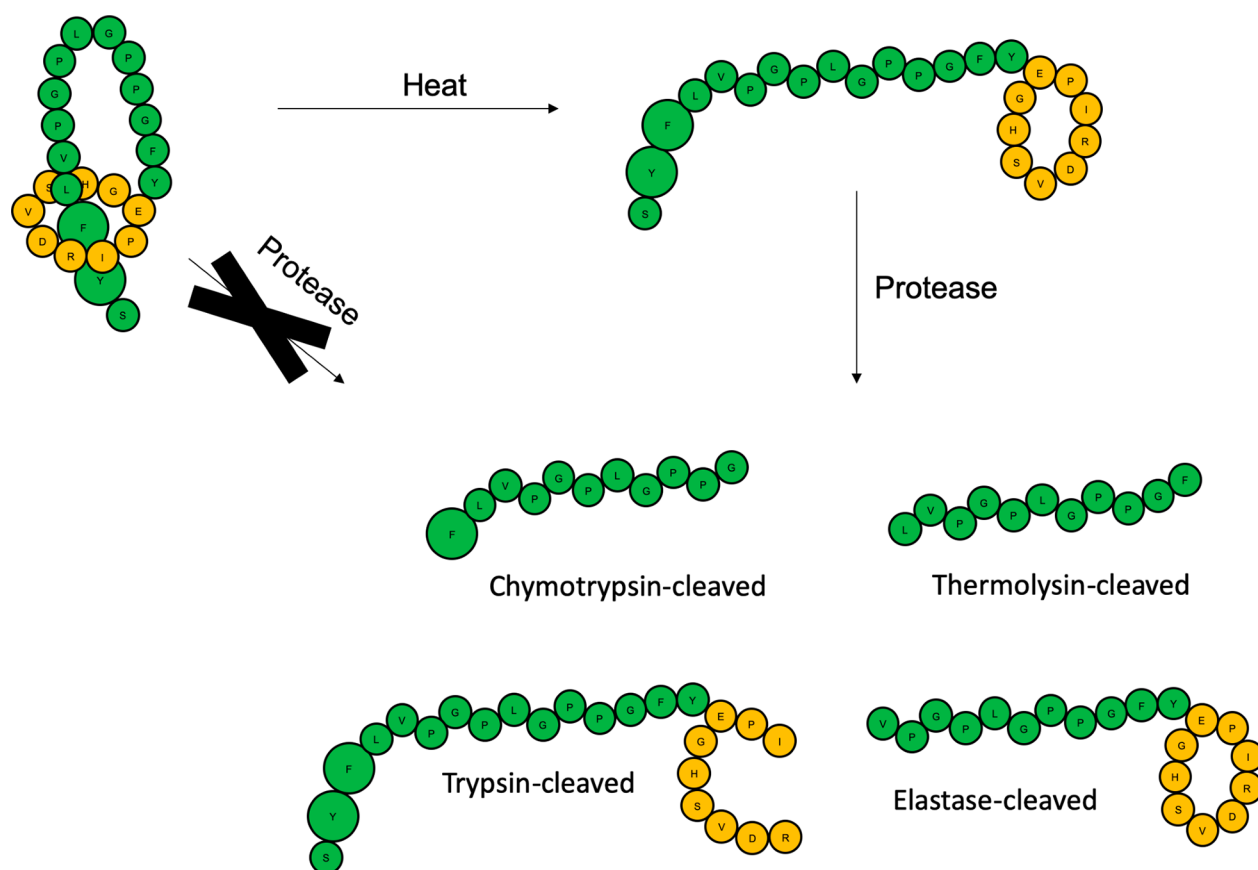
Figure 4. Threaded cloacaenodin is resistant to proteolysis while the unthreaded conformer is proteolyzed into the major products shown. Loop/tail residues are colored green and ring residues are colored orange. Phe22 and Tyr23 are enlarged to denote their role as the steric lock residues for cloacaenodin. The LC−MS data underlying this schematic are shown in Figures S13−S16.

demonstrated that the amide proton shifts for unthreaded lasso peptides are generally in a narrower range.[51]

The 150 ms NOESY spectrum was integrated for through-space distance restraints. From the NOESY spectrum, we observed interactions between protons from Phe22 with Asp5, Arg6, Pro8, and Glu9, as well as between protons from Tyr23 with Gly1, His2, Asp5, Ile7, Pro8, and Glu9 (Table S9). These interactions indicated that Phe22 and Ty23 likely function as the bulky steric lock residues to keep the peptide threaded. Our assignments as well as through-space NOEs from integrated peaks and explicit distance constraints around the isopeptide bond (calculated from the rubrivinodin crystal structure PDB 5OQZ)[53] were given to CYANA 2.1[54] using the automated mode, where all prolines were presumed *trans*.

The top 20 structures calculated by CYANA show Phe22 and Tyr23 as the upper and lower steric lock residues, respectively (Figure 3A), similar to the Phe19 and Tyr20 steric locks of MccJ25.[50,55,56] Cloacaenodin has a loop region of 13 amino acids, which is the second largest loop observed after ubonodin, and a short tail of only two amino acids (Figure 3B). This large loop and short tail structure is similar to the RNAP-inhibiting lasso peptides MccJ25, ubonodin, citrocin, klebsidin, and acinetodin, but with cloacaenodin being unique with its C-terminal serine and 9-membered ring (Figure S12).

Threaded Cloacaenodin Resists Protease Cleavage. One of the advantages of lasso peptides is that they are often resistant to proteolysis. We previously established that cloacaenodin was resistant to C-terminal proteolysis by the exopeptidase carboxypeptidase (Figure S3−S4), and we

wanted to see if this peptide would be resistant to endopeptidases.

The sequence of cloacaenodin contains residues cleavable by trypsin, chymotrypsin, elastase, and thermolysin. As expected, when we tested a sample of unthreaded cloacaenodin (generated by heating), we observed fragments consistent with cleavage of the unthreaded peptide both in its linear and ring segments. In stark contrast, under the same conditions, the threaded peptide remained resistant to proteolysis by each of these four proteases (Figures 4 and S13−S16). This is consistent with the reported proteolytic resistance of previously discovered lasso peptides and demonstrates that the threaded structure of cloacaenodin is essential to its proteolytic stability.[57−59]

Cloacaenodin Has Antimicrobial Activity against Multiple *Enterobacter* Strains. After characterizing the structure and proteolytic resistance of cloacaenodin, we next tested if cloacaenodin could inhibit bacterial growth. As a preliminary test of antimicrobial activity, we cloned a version of our expression plasmid where the *cloD* gene was removed, so that the lasso peptide could not be exported by the *E. coli* upon IPTG-induced expression. We found that *E. coli* XL-1 Blue colonies did not appear on LB agar when IPTG was added to the plate (Figure S17), indicative of intracellular cloacaenodin toxicity.

Of the antimicrobial lasso peptides characterized to date, most target strains that are phylogenetically or environmentally related to the producing strain.[60] Therefore, we chose to test strains that were members of the ECC as well as strains that

may reside in the same environmental niche as *Enterobacter* strains. We acknowledge that there are different proposed names for some of the strains we tested, such as the reclassification of *E. amnigenus* and *E. nimipressuralis* to the genus *Lelliottia*.[61]

We used spot-on-lawn assays in M63 agar against a panel of bacteria using purified cloacaenodin dissolved in water (Figure S18A, Table S4A). Cloacaenodin had no observed activity against *E. coli* MG1655, *B. subtilis* 168, *Salmonella enterica* serovar Newport, *Klebsiella aerogenes* ATCC 13048, *Enterobacter hormaechei* ATCC 700323, and *Enterobacter kobei* BAA-260. However, we observed zones of inhibition in the low micromolar range when we tested cloacaenodin against *E. cloacae* ATCC 13047, *E. mori* DSM 26271, *E. asburiae* DSM 17506, *E. amnigenus* ATCC 33072, and *E. nimipressuralis* DSM 18955 (Table 1). *E. cloacae* is the most clinically relevant strain

Table 1. Minimal Inhibitory Concentration (MIC) of Cloacaenodin against Susceptible Strains[a]

species	MIC in M63 media
Enterobacter cloacae ATCC 13047	7.5 μM (agar)/940 nM (liquid)
E. nimipressuralis DSM 18955	1.9 μM (agar)
E. asburiae DSM 17506	3.8 μM (agar)
E. mori DSM 26271	1.9 μM (agar)
E. amnigenus ATCC 33072	500 nM (agar)/230 nM (liquid)
E. cloacae UCI102	1.0 μM (agar)
E. ludwigii MGH216	1.0 μM (agar)
E. kobei MGH178	2.0 μM (agar)
E. hormaechei UCI35	2.0 μM (agar)
E. asburiae MGH243	1.0 μM (agar)
E. asburiae UCI193	1.0 μM (agar)

[a]Asterisk indicates that the strain is a clinical isolate.

that we found activity against, as this pathogen is a frequent cause of nosocomial infections around the globe.[2] The other strains that we found as susceptible to cloacaenodin are known to be causative agents for certain plant diseases or occasional human pathogens.[62−65]

The type strain of *E. cloacae* (ATCC 13047) tested above was isolated from human cerebrospinal fluid in 1890[66] before the era of antibiotics. We were motivated to test whether cloacaenodin would have activity against more recent clinical isolates. We tested a panel of 12 clinical isolates of *Enterobacter* using the spot-on-lawn assay (Table S4B). These isolates are part of a larger collection of carbapenem-resistant *Enterobacterales* (CRE) that have been extensively analyzed for their genetic mechanisms of resistance.[67] In 6 of these strains, 3 of which are classified as resistant to carbapenem antibiotics, we consistently observed low micromolar values of the minimal inhibitory concentration (MIC) of cloacaenodin (Table 1, Figure S18B). In the other 6 clinical isolates (Table S4B), we observed either weak or no activity. The observation of strain-specific activity is consistent with the observed narrow-spectrum activity of ubonodin against *Burkholderia* strains due to transport through PupB.[16,68] These assays demonstrate that cloacaenodin has the potential to serve as a potent therapeutic against *Enterobacter* strains that have evolved resistance to last-resort antibiotics.

We also tested the bioactivity of a sample of cloacaenodin that had been heated and then HPLC-purified to isolate the unthreaded peptide. At a concentration of 15 μM, we observed no activity of this unthreaded peptide against *E. cloacae*,

consistent with our understanding of the essential nature of the threaded structure for activity (Figure S19).

Cloacaenodin was also tested against *E. cloacae* and *E. amnigenus* using a broth microdilution assay in M63 media. We observed an MIC value of 940 nM for *E. cloacae* and 230 nM for *E. amnigenus* from this assay, showing that cloacaenodin is more active in solution than on solid media (Table 1, Figure S20). When testing against *E. cloacae*, we noticed larger OD values for sub-MIC treated wells, which motivated us to see if there was a phenotypic abnormality for these cells. When looking at some of the treated bacteria under the microscope, we observed that *E. cloacae* cells that were treated with sub-MIC values of cloacaenodin exhibited a degree of filamentation (Figure S21). Filamentation has previously been observed for *E. coli* cells upon exposure to MccJ25.[13]

Stability and Bioactivity of Cloacaenodin Variants. To gain insight into the contribution of specific cloacaenodin residues toward its stability and bioactivity, we carried out site-directed mutagenesis on various residues, with the main results summarized in Table 2. We were intrigued by the fact that we

Table 2. Summary of Yield, Stability, and Bioactivity of Cloacaenodin Variants[a]

cloacaenodin variant	yield relative to WT	stability relative to WT	bioactivity relative to WT
F22W	++	comparable	comparable
Y23W	+	more	n.d.
S24G	+++	less	abolished
S24T	++	comparable	less
S24C	++	comparable	less
S24A	++	comparable	comparable
S24Y	++	comparable	comparable
10-membered ring	L	less	n.d.
G1A	not tolerated	N/A	N/A
E9D	not tolerated	N/A	N/A
P8A	++	comparable	n.d.
V4P	L	more	n.d.
Y10A	+	comparable	much less

[a]For yield, +++ signifies made at near wild-type levels, ++ signifies made at ~40−60% wild-type levels, + signifies made at ≤10% wild-type levels, all as detected by absorbance at UV-215 measured from HPLC. L signifies only detected via LC−MS. Stability was judged by ratio of threaded-to-unthreaded peptide in supernatant extract after purification, judged by LC−MS. N/A stands for not applicable. Variants that were not tested for bioactivity are listed as n.d. for no data.

saw a peak of unthreaded cloacaenodin in the supernatant extract (Figure S2). We reasoned that increasing the side chain volume of the steric lock residues Phe22 and Tyr23 may retard the unthreading process. Swapping of the upper steric lock Phe22 to Trp still resulted in comparable levels of unthreaded peptide in the extract, while a Y23W variant only had the threaded peptide observable in its supernatant extract (although the yield was reduced >10-fold) (Figure S22).

Since cloacaenodin is unique in having a C-terminal serine compared to other lasso peptides that inhibit RNAP, we next swapped this residue to the more typical C-terminal glycine. To our surprise, when we expressed the S24G variant, we found that the majority of the peptide was now unthreaded in the supernatant extract, based on the later retention time as well as heating and carboxypeptidase assays (Figure S23). This

unthreaded peptide completely lost bioactivity when tested against *E. amnigenus* (Figure S24). However, when expressed intracellularly without the *cloD* gene present, the S24G variant still inhibited *E. coli* cell growth, suggesting that at least some fraction of the peptide remains threaded in the cytoplasm and exerts antimicrobial activity (Figure S25). Surprised by the S24G results, we next made conservative substitutions to the S24 residue (cloacaenodin S24A, S24C, and S24T), all of which were similarly stable to wild-type and had similar or decreased bioactivity compared to wild-type (Figure S24). Given the unthreading behavior, we hypothesized swapping the S24 to a bulkier Tyr, Phe, or Trp residue may stabilize the lassoed shape, but we found that these variants still allowed unthreading. The S24Y mutant was purified by HPLC and had similar bioactivity as wild-type (Figure S24).

We next asked if the cloacaenodin biosynthetic enzymes could tolerate an increase in ring size. An increase in ring size from 9 to 10 aa was previously reported for the lasso peptide fuscanodin/fusilassin.[69] We cloned a variant of cloacaenodin with an extra alanine near the middle of the ring, so that the new ring sequence would be GHSVA**A**DRIPE. We detected a single peak corresponding to the expected mass and isotopic distribution in the supernatant, eluting at about 12.1 min, made at about 1% of the yield as wild-type. Heating assays and carboxypeptidase assays of the extract demonstrated that this was an unthreaded peptide (Figure S26). We hypothesize that the lasso peptide is first made threaded by the B and C enzymes, but then readily unthreads upon being secreted into the supernatant and during our purification procedure (Figure S27).

While changes to the isopeptide-bonded residues are generally not tolerated for lasso peptides,[70,71] several reports demonstrated that certain biosynthetic enzymes could tolerate variations at these positions.[23,72,73] For cloacaenodin, G1A and E9D variants were not produced, as the variants could not be detected in the supernatant or the cell pellet.

A report by Hegemann et al. demonstrated that a proline at position 8 in the 9-membered ring of the lasso peptide caulosegnin II was vital for prevention of unthreading at 95 °C.[74] For cloacaenodin, we did not observe a dramatic decrease in the ratio of threaded-to-unthreaded peptide in the extract for a cloacaenodin P8A variant (Figure S28). However, swapping the Val4 residue to Pro appeared to favor the threaded peptide, suggesting that rigidification of the ring with proline can stabilize the lasso peptide against unthreading. This increased stability comes at a cost, however, as the V4P variant is only made at about 1% of the wild-type yield (Figure S29).

The Tyr9 side chain in MccJ25 (corresponding to Tyr10 in cloacaenodin) was shown to hydrogen bond with RNA polymerase in a cocrystal structure.[40] We purified a cloacaenodin Y10A variant but found that, despite being threaded, it had drastically reduced activity against *E. amnigenus* (Figure S30). When expressing this peptide in *E. coli* without CloD present, the *E. coli* cells could still grow, suggesting that the Y10A variant lacks activity due to decreased target binding as opposed to decreased transport into susceptible cells (Figure S17).

DISCUSSION AND CONCLUSION

This paper focuses on a novel antimicrobial lasso peptide cloacaenodin. This lasso peptide is particularly notable because of its potent antimicrobial activity against multiple members of the *Enterobacter* genus, including those implicated in

nosocomial infections. While other lasso peptides with antimicrobial activity against Gram-negative bacteria such as klebsidin, capistruin, and citrocin have only modest potency, the MIC of cloacaenodin is in the high nanomolar to single micromolar range for the strains tested here. This potency coupled with the urgency to develop new antimicrobial interventions against the ESKAPE pathogen *Enterobacter* makes cloacaenodin a promising lead for antibiotic development. We noted that BGCs related to cloacaenodin are present in 5 different species of *Enterobacter* as well as other enterobacteria (Figure S1). Furthermore, many of the BGCs appear in genomic contexts consistent with being plasmid-borne. The mobility of the cloacaenodin BGC may be due to horizontal gene transfer between these strains which are all part of the gut microbiota. We speculate this horizontal gene transfer occurs because cloacaenodin confers a competitive advantage on the producing cells.

We were initially interested in cloacaenodin not only because of its antimicrobial potential but also because it differs in structure from other antimicrobial lasso peptides targeting Gram-negative bacteria. Specifically, cloacaenodin has a 9-membered ring and a C-terminal serine, in contrast to other characterized examples which have 8-membered rings and C-terminal glycine (Figure 1). Cloacaenodin is also unusually rich in proline residues with 5 prolines, 4 of which are in the 13 aa loop region. As we noted above, the threaded structure of cloacaenodin protects it from proteolysis (Figure 4). The high prevalence of prolines in the structure likely contributes to this proteolytic resistance as well. Proline *cis/trans* isomerization is known in lasso peptides,[75] and so in principle cloacaenodin may exist as an ensemble of up to 32 (ie 2^5) different conformers. In addition to the likely role of proline in engendering cloacaenodin with proteolytic resistance, this conformational flexibility may also be related to the antimicrobial activity.

METHODS

Detailed materials and methods used in this study can be found in the Supporting Information.

Cloacaenodin BGC Identification. The cloacaenodin BGC was found through a precursor-centric genome mining approach,[26] where we prioritized hits having a Tyr after the ring as well as a penultimate Tyr. Subsequent BlastP searches were conducted on the *cloA* gene to identify cloacaenodin-like BGCs in other strains.

Plasmid Construction. For heterologous expression in *E. coli*, the cloacaenodin BGC was refactored and cloned into the pQE-80 vector. Primers were used to assemble the *cloA* gene which is under the control of the T5 promoter, and synthesized gBlocks were used to assemble the *cloBCD* genes which are under the control of the promoter for *mcjBCD*. Mutagenic primers were used to generate plasmids to express cloacaenodin variants.

Heterologous Expression and Purification. To generate cloacaenodin and cloacaenodin variants, we used *E. coli* BL-21 which had been transformed via electroporation with a plasmid to express cloacaenodin or a given variant. The transformed cells were grown at 37 °C with shaking in M9 minimal media (containing M9 salts supplemented with glucose, $MgSO_4$, thiamine, and amino acids) with 100 μg/mL ampicillin. Once the OD_{600} of the culture reached ~0.2, 1 mM IPTG was added to the culture, which was then allowed

to continue growing at room temperature with shaking overnight.

Following expression, the cultures were centrifuged to isolate the supernatant. The supernatant was further purified via a C8 column and eluted with methanol. The methanol extract was dried via rotary evaporation, and the dried extract was resuspended in water (1 mL/L of culture).

The resuspended extracts were purified via HPLC, and masses were verified via LC−MS analysis. Some peptide variants expressed too poorly for HPLC analysis, so they were instead only analyzed via LC−MS. The cloacaenodin Y10A variant required a second round of HPLC purification before use in antimicrobial assays. HPLC-purified peptides were lyophilized before use in later assays.

NMR Data Acquisition and Determination of Cloacaenodin Structure. We acquired NMR spectra, including TOCSY and two NOESY spectra (300 and 150 ms mixing time), at the Princeton University Department of Chemistry NMR Facility. We maintained the sample at 4 °C during acquisition to ensure that cloacaenodin remained threaded. Following data acquisition, MNova was used for residue assignment, and through-space distance restraints were manually chosen from the 150 ms mixing time NOESY spectrum. With these residue assignments and distance restraints, CYANA 2.1 was employed to generate 20 structures of cloacaenodin. Each of the 20 structures was then energy minimized with Avogadro.

Evaluation of Antimicrobial Activity. Purified cloacaenodin was dissolved in water and its concentration measured by determining its absorbance at 280 nm using a NanoDrop instrument. A spot-on-lawn assay was employed to evaluate antimicrobial activity against a panel of strains. A strain of interest was cultured overnight in LB media. This culture was then used to inoculate 5 mL of LB, which was grown until midexponential phase ($OD_{600} \approx 0.4-0.6$). The culture was then used to inoculate 10 mL of melted M63 soft agar at an inoculum of $\sim 10^7$ CFUs/mL. The soft agar was poured atop a plate with 10 mL of M63 agar and allowed to dry. Dissolved cloacaenodin (10 μL) was spotted on the plate at various concentrations and then allowed to dry on the plate. After incubation of the plate overnight, the plate was analyzed for zones of inhibition. The last visible spot was defined as the MIC.

For *E. cloacae* and *E. amnigenus*, a broth microdilution assay in M63 media was also used to evaluate antimicrobial activity. The same procedure above was followed, but instead of inoculating M63 soft agar, the culture was used to inoculate liquid cultures (starting OD_{600} of 0.0005) in a 96-well plate. The plates were then grown with shaking and their OD_{600} was measured after 8 and 16 h. The lowest concentration with no visible bacterial growth was defined as the MIC. For some of the cultures grown in the plate at sub-MIC concentrations, microscopy was employed to view the morphology of the bacteria.

Proteolytic Susceptibility Assays. Cloacaenodin (or a variant) was incubated with carboxypeptidase B and carboxypeptidase Y at 20 °C for 16 h in a buffer of 50 mM sodium acetate, pH 6.0. For trypsin digestion, cloacaenodin was incubated in 50 mM ammonium bicarbonate buffer with trypsin in a 1:100 trypsin:peptide weight ratio. The reaction proceeded for 30 min to 1 h before quenching. For α-chymotrypsin digestion, cloacaenodin was incubated in a buffer of 100 mM Tris, 10 mM CaCl$_2$, pH 8.0, with 0.04 mg/mL α-chymotrypsin. The reaction proceeded for 1 h at 25 °C before quenching. For elastase digestion, cloacaenodin was incubated in a buffer of 50 mM Tris, pH 9.0, with 0.04 mg/mL elastase. The reaction proceeded for 1 h at 25 °C before quenching. For thermolysin digestion, cloacaenodin was incubated in a buffer of 50 mM Tris, 0.5 mM CaCl$_2$, pH 8.0 with 0.04 mg/mL thermolysin. The reaction proceeded for 1 h at 30 °C before quenching. All reactions were quenched via addition of 1% formic acid.

■ ASSOCIATED CONTENT

ⓢ Supporting Information

The Supporting Information is available free of charge at https://pubs.acs.org/doi/10.1021/acsinfecdis.2c00446.

Detailed experimental methods and materials, including details on cloacaenodin BGC identification, cloacaenodin heterologous expression, NMR analysis, antimicrobial assays, and protease assays (PDF)

■ AUTHOR INFORMATION

Corresponding Author

A. James Link − *Department of Chemical and Biological Engineering, Princeton University, Princeton, New Jersey 08544, United States; Department of Molecular Biology and Department of Chemistry, Princeton University, Princeton, New Jersey 08544, United States;* ⓞ orcid.org/0000-0001-5066-9691; Email: ajlink@princeton.edu

Authors

Drew V. Carson − *Department of Chemical and Biological Engineering, Princeton University, Princeton, New Jersey 08544, United States;* ⓞ orcid.org/0000-0002-4209-2199

Monica Patiño − *Department of Chemical and Biological Engineering, Princeton University, Princeton, New Jersey 08544, United States*

Hader E. Elashal − *Department of Chemical and Biological Engineering, Princeton University, Princeton, New Jersey 08544, United States*

Alexis Jaramillo Cartagena − *Infectious Disease and Microbiome Program, Broad Institute of MIT and Harvard, Cambridge, Massachusetts 02142, United States*

Yi Zhang − *Department of Chemical and Biological Engineering, Princeton University, Princeton, New Jersey 08544, United States*

Megan E. Whitley − *Department of Chemical and Biological Engineering, Princeton University, Princeton, New Jersey 08544, United States*

Larry So − *Department of Chemical and Biological Engineering, Princeton University, Princeton, New Jersey 08544, United States;* ⓞ orcid.org/0000-0001-8863-7601

Angelo K. Kayser-Browne − *Department of Molecular Biology, Princeton University, Princeton, New Jersey 08544, United States*

Ashlee M. Earl − *Infectious Disease and Microbiome Program, Broad Institute of MIT and Harvard, Cambridge, Massachusetts 02142, United States*

Roby P. Bhattacharyya − *Infectious Disease and Microbiome Program, Broad Institute of MIT and Harvard, Cambridge, Massachusetts 02142, United States; Infectious Diseases Division, Department of Medicine, Massachusetts General Hospital, Boston, Massachusetts 02114, United States;* ⓞ orcid.org/0000-0001-6955-5088

Complete contact information is available at:
https://pubs.acs.org/10.1021/acsinfecdis.2c00446

Notes

■ ACKNOWLEDGMENTS

■ REFERENCES

(1) Pendleton, J. N.; Gorman, S. P.; Gilmore, B. F. Clinical Relevance of the ESKAPE Pathogens. *Expert Rev. Anti-Infe.* **2013**, *11* (3), 297−308.

(2) Davin-Regli, A.; Pagès, J.-M. *Enterobacter aerogenes* and *Enterobacter cloacae*; Versatile Bacterial Pathogens Confronting Antibiotic Treatment. *Front. Microbiol.* **2015**, *6*, 392.

(3) Annavajhala, M. K.; Gomez-Simmonds, A.; Uhlemann, A.-C. Multidrug-Resistant *Enterobacter cloacae* Complex Emerging as a Global, Diversifying Threat. *Front. Microbiol.* **2019**, *10*, 44.

(4) Mezzatesta, M. L.; Gona, F.; Stefani, S. *Enterobacter cloacae* Complex: Clinical Impact and Emerging Antibiotic Resistance. *Future Microbiol.* **2012**, *7* (7), 887−902.

(5) Davin-Regli, A.; Lavigne, J.-P.; Pagès, J.-M. *Enterobacter* Spp.: Update on Taxonomy, Clinical Aspects, and Emerging Antimicrobial Resistance. *Clin. Microbiol. Rev.* **2019**, *32* (4), e00002-19.

(6) Bialvaei, A. Z.; Kafil, H. S. Colistin, Mechanisms and Prevalence of Resistance. *Curr. Med. Res. Opin.* **2015**, *31* (4), 707−721.

(7) Nation, R. L.; Li, J. Colistin in the 21st Century. *Curr. Opin. Infect. Dis.* **2009**, *22* (6), 535−543.

(8) Zong, Z.; Feng, Y.; McNally, A. Carbapenem and Colistin Resistance in *Enterobacter*: Determinants and Clones. *Trends Microbiol.* **2021**, *29* (6), 473−476.

(9) Norgan, A. P.; Freese, J. M.; Tuin, P. M.; Cunningham, S. A.; Jeraldo, P. R.; Patel, R. Carbapenem- and Colistin-Resistant *Enterobacter cloacae* from Delta, Colorado, in 2015. *Antimicrob. Agents Ch.* **2016**, *60* (5), 3141−3144.

(10) Zeng, K.-J.; Doi, Y.; Patil, S.; Huang, X.; Tian, G.-B. Emergence of the Plasmid-Mediated *mcr-1* Gene in Colistin-Resistant *Enterobacter aerogenes* and *Enterobacter cloacae*. *Antimicrob. Agents Ch.* **2016**, *60* (6), 3862−3863.

(11) Kang, K. N.; Klein, D. R.; Kazi, M. I.; Guérin, F.; Cattoir, V.; Brodbelt, J. S.; Boll, J. M. Colistin Heteroresistance in *Enterobacter cloacae* Is Regulated by PhoPQ-Dependent 4-Amino-4-Deoxy-l-Arabinose Addition to Lipid A. *Mol. Microbiol.* **2019**, *111* (6), 1604−1616.

(12) Liao, W.; Cui, Y.; Quan, J.; Zhao, D.; Han, X.; Shi, Q.; Wang, Q.; Jiang, Y.; Du, X.; Li, X.; Yu, Y. High Prevalence of Colistin Resistance and *mcr-9/10* Genes in *Enterobacter* Spp. in a Tertiary Hospital over a Decade. *Int. J. Antimicrob. Ag.* **2022**, *59* (5), 106573.

(13) Salomón, R. A.; Farías, R. N. Microcin 25, a Novel Antimicrobial Peptide Produced by *Escherichia coli*. *J. Bacteriol.* **1992**, *174* (22), 7428−7435.

(14) Knappe, T. A.; Linne, U.; Zirah, S.; Rebuffat, S.; Xie, X.; Marahiel, M. A. Isolation and Structural Characterization of Capistruin, a Lasso Peptide Predicted from the Genome Sequence of *Burkholderia thailandensis* E264. *J. Am. Chem. Soc.* **2008**, *130* (34), 11446−11454.

(15) Iwatsuki, M.; Uchida, R.; Takakusagi, Y.; Matsumoto, A.; Jiang, C.-L.; Takahashi, Y.; Arai, M.; Kobayashi, S.; Matsumoto, M.; Inokoshi, J.; Tomoda, H.; Omura, S. Lariatins, Novel Anti-Mycobacterial Peptides with a Lasso Structure, Produced by *Rhodococcus jostii* K01-B0171. *J. Antibiot.* **2007**, *60* (6), 357−363.

(16) Cheung-Lee, W. L.; Parry, M. E.; Zong, C.; Cartagena, A. J.; Darst, S. A.; Connell, N. D.; Russo, R.; Link, A. J. Discovery of Ubonodin, an Antimicrobial Lasso Peptide Active against Members of the *Burkholderia cepacia* Complex. *Chembiochem* **2020**, *21* (9), 1335−1340.

(17) Cheung-Lee, W. L.; Parry, M. E.; Cartagena, A. J.; Darst, S. A.; Link, A. J. Discovery and Structure of the Antimicrobial Lasso Peptide Citrocin. *J. Biol. Chem.* **2019**, *294* (17), 6822−6830.

(18) Tsunakawa, M.; Hu, S.-L.; Hoshino, Y.; Detlefson, D. J.; Hill, S. E.; Furumai, T.; White, R. J.; Nishio, M.; Kawano, K.; Yamamoto, S.; Fukagawa, Y.; Oki, T. Siamycins I and II, New Anti-HIV Peptides: I. Fermentation, Isolation, Biological Activity and Initial Characterization. *J. Antibiot.* **1995**, *48* (5), 433−434.

(19) Metelev, M.; Arseniev, A.; Bushin, L. B.; Kuznedelov, K.; Artamonova, T. O.; Kondratenko, R.; Khodorkovskii, M.; Seyedsayamdost, M. R.; Severinov, K. Acinetodin and Klebsidin, RNA Polymerase Targeting Lasso Peptides Produced by Human Isolates of *Acinetobacter gyllenbergii* and *Klebsiella pneumoniae*. *ACS Chem. Biol.* **2017**, *12* (3), 814−824.

(20) Metelev, M.; Tietz, J. I.; Melby, J. O.; Blair, P. M.; Zhu, L.; Livnat, I.; Severinov, K.; Mitchell, D. A. Structure, Bioactivity, and Resistance Mechanism of Streptomonomicin, an Unusual Lasso Peptide from an Understudied Halophilic Actinomycete. *Chem. Biol.* **2015**, *22* (2), 241−250.

(21) Gavrish, E.; Sit, C. S.; Cao, S.; Kandror, O.; Spoering, A.; Peoples, A.; Ling, L.; Fetterman, A.; Hughes, D.; Bissell, A.; Torrey, H.; Akopian, T.; Mueller, A.; Epstein, S.; Goldberg, A.; Clardy, J.; Lewis, K. Lassomycin, a Ribosomally Synthesized Cyclic Peptide, Kills *Mycobacterium tuberculosis* by Targeting the ATP-Dependent Protease ClpC1P1P2. *Chem. Biol.* **2014**, *21* (4), 509−518.

(22) Stariha, L. M.; McCafferty, D. G. Discovery of the Class I Antimicrobial Lasso Peptide Arcumycin. *Chembiochem* **2021**, *22* (16), 2632−2640.

(23) Li, Y.; Ducasse, R.; Zirah, S.; Blond, A.; Goulard, C.; Lescop, E.; Giraud, C.; Hartke, A.; Guittet, E.; Pernodet, J.-L.; Rebuffat, S. Characterization of Sviceucin from *Streptomyces* Provides Insight into Enzyme Exchangeability and Disulfide Bond Formation in Lasso Peptides. *ACS Chem. Biol.* **2015**, *10* (11), 2641−2649.

(24) Shao, M.; Ma, J.; Li, Q.; Ju, J. Identification of the Anti-Infective Aborycin Biosynthetic Gene Cluster from Deep-Sea-Derived *Streptomyces* sp. SCSIO ZS0098 Enables Production in a Heterologous Host. *Mar. Drugs* **2019**, *17* (2), 127.

(25) Montalbán-López, M.; Scott, T. A.; Ramesh, S.; Rahman, I. R.; van Heel, A. J.; Viel, J. H.; Bandarian, V.; Dittmann, E.; Genilloud, O.; Goto, Y.; Burgos, M. J. G.; Hill, C.; Kim, S.; Koehnke, J.; Latham, J. A.; Link, A. J.; Martínez, B.; Nair, S. K.; Nicolet, Y.; Rebuffat, S.; Sahl, H.-G.; Sareen, D.; Schmidt, E. W.; Schmitt, L.; Severinov, K.; Süssmuth, R. D.; Truman, A. W.; Wang, H.; Weng, J.-K.; van Wezel, G. P.; Zhang, Q.; Zhong, J.; Piel, J.; Mitchell, D. A.; Kuipers, O. P.; van der Donk, W. A. New Developments in RiPP Discovery, Enzymology and Engineering. *Nat. Prod. Rep.* **2021**, *38* (1), 130−239.

(26) Maksimov, M. O.; Pelczer, I.; Link, A. J. Precursor-Centric Genome-Mining Approach for Lasso Peptide Discovery. *Proc. Natl. Acad. Sci. U. S. A.* **2012**, *109* (38), 15223−15228.

(27) Duquesne, S.; Destoumieux-Garzón, D.; Zirah, S.; Goulard, C.; Peduzzi, J.; Rebuffat, S. Two Enzymes Catalyze the Maturation of a Lasso Peptide in *Escherichia coli*. *Chem. Biol.* **2007**, *14* (7), 793−803.

(28) Yan, K.-P.; Li, Y.; Zirah, S.; Goulard, C.; Knappe, T. A.; Marahiel, M. A.; Rebuffat, S. Dissecting the Maturation Steps of the Lasso Peptide Microcin J25 in Vitro. *Chembiochem* **2012**, *13* (7), 1046−1052.

(29) Cheung-Lee, W. L.; Link, A. J. Genome Mining for Lasso Peptides: Past, Present, and Future. *J. Ind. Microbiol. Biot.* **2019**, *46* (9−10), 1371−1379.

(30) Kloosterman, A. M.; Cimermancic, P.; Elsayed, S. S.; Du, C.; Hadjithomas, M.; Donia, M. S.; Fischbach, M. A.; van Wezel, G. P.; Medema, M. H. Expansion of RiPP Biosynthetic Space through Integration of Pan-Genomics and Machine Learning Uncovers a Novel Class of Lanthipeptides. *PLOS Biol.* **2020**, *18* (12), No. e3001026.

(31) Agrawal, P.; Khater, S.; Gupta, M.; Sain, N.; Mohanty, D. RiPPMiner: A Bioinformatics Resource for Deciphering Chemical Structures of RiPPs Based on Prediction of Cleavage and Cross-Links. *Nucleic Acids Res.* **2017**, *45* (W1), W80−W88.

(32) Kloosterman, A. M.; Shelton, K. E.; van Wezel, G. P.; Medema, M. H.; Mitchell, D. A. RRE-Finder: A Genome-Mining Tool for Class-Independent RiPP Discovery. *mSystems* **2020**, *5* (5), No. e00267-20.

(33) Zhong, Z.; He, B.; Li, J.; Li, Y.-X. Challenges and Advances in Genome Mining of Ribosomally Synthesized and Post-Translationally Modified Peptides (RiPPs). *Synthetic Syst. Biotechnology* **2020**, *5* (3), 155−172.

(34) de los Santos, E. L. C. NeuRiPP: Neural Network Identification of RiPP Precursor Peptides. *Sci. Rep.* **2019**, *9* (1), 13406.

(35) Russell, A. H.; Truman, A. W. Genome Mining Strategies for Ribosomally Synthesised and Post-Translationally Modified Peptides. *Comput. Struct. Biotechnology J.* **2020**, *18*, 1838−1851.

(36) Li, Y.; Rebuffat, S. The Manifold Roles of Microbial Ribosomal Peptide−Based Natural Products in Physiology and Ecology. *J. Biol. Chem.* **2020**, *295* (1), 34−54.

(37) Rebuffat, S. Ribosomally Synthesized Peptides, Foreground Players in Microbial Interactions: Recent Developments and Unanswered Questions. *Nat. Prod. Rep.* **2022**, *39* (2), 273−310.

(38) Cao, L.; Do, T.; Link, A. J. Mechanisms of Action of Ribosomally Synthesized and Posttranslationally Modified Peptides (RiPPs). *J. Ind. Microbiol. Biot.* **2021**, *48* (3−4), kuab005.

(39) Granato, E. T.; Meiller-Legrand, T. A.; Foster, K. R. The Evolution and Ecology of Bacterial Warfare. *Curr. Biol.* **2019**, *29* (11), R521−R537.

(40) Braffman, N. R.; Piscotta, F. J.; Hauver, J.; Campbell, E. A.; Link, A. J.; Darst, S. A. Structural Mechanism of Transcription Inhibition by Lasso Peptides Microcin J25 and Capistruin. *Proc. Natl. Acad. Sci. U. S. A.* **2019**, *116* (4), 1273−1278.

(41) Solbiati, J. O.; Ciaccio, M.; Farías, R. N.; González-Pastor, J. E.; Moreno, F.; Salomón, R. A. Sequence Analysis of the Four Plasmid Genes Required To Produce the Circular Peptide Antibiotic Microcin J25. *J. Bacteriol.* **1999**, *181* (8), 2659−2662.

(42) Mukhopadhyay, J.; Sineva, E.; Knight, J.; Levy, R. M.; Ebright, R. H. Antibacterial Peptide Microcin J25 Inhibits Transcription by Binding within and Obstructing the RNA Polymerase Secondary Channel. *Mol. Cell* **2004**, *14* (6), 739−751.

(43) Adelman, K.; Yuzenkova, J.; La Porta, A.; Zenkin, N.; Lee, J.; Lis, J. T.; Borukhov, S.; Wang, M. D.; Severinov, K. Molecular Mechanism of Transcription Inhibition by Peptide Antibiotic Microcin J25. *Mol. Cell* **2004**, *14* (6), 753−762.

(44) Kirsch, S. H.; Haeckl, F. P. J.; Müller, R. Beyond the Approved: Target Sites and Inhibitors of Bacterial RNA Polymerase from Bacteria and Fungi. *Nat. Prod. Rep.* **2022**, *39* (6), 1226−1263.

(45) Pan, S. J.; Cheung, W. L.; Link, A. J. Engineered Gene Clusters for the Production of the Antimicrobial Peptide Microcin J25. *Protein Expres. Purif.* **2010**, *71* (2), 200−206.

(46) Hegemann, J. D.; Zimmermann, M.; Zhu, S.; Klug, D.; Marahiel, M. A. Lasso Peptides from Proteobacteria: Genome Mining Employing Heterologous Expression and Mass Spectrometry. *Biopolymers* **2013**, *100* (5), 527−542.

(47) Koos, J. D.; Link, A. J. Heterologous and *in Vitro* Reconstitution of Fuscanodin, a Lasso Peptide from *Thermobifida fusca*. *J. Am. Chem. Soc.* **2019**, *141* (2), 928−935.

(48) Allen, C. D.; Chen, M. Y.; Trick, A. Y.; Le, D. T.; Ferguson, A. L.; Link, A. J. Thermal Unthreading of the Lasso Peptides Astexin-2 and Astexin-3. *ACS Chem. Biol.* **2016**, *11* (11), 3043−3051.

(49) Hegemann, J. D. Factors Governing the Thermal Stability of Lasso Peptides. *Chembiochem* **2020**, *21* (1−2), 7−18.

(50) Wilson, K.-A.; Kalkum, M.; Ottesen, J.; Yuzenkova, J.; Chait, B. T.; Landick, R.; Muir, T.; Severinov, K.; Darst, S. A. Structure of Microcin J25, a Peptide Inhibitor of Bacterial RNA Polymerase, Is a Lassoed Tail. *J. Am. Chem. Soc.* **2003**, *125* (41), 12475−12483.

(51) Xie, X.; Marahiel, M. A. NMR as an Effective Tool for the Structure Determination of Lasso Peptides. *Chembiochem* **2012**, *13* (5), 621−625.

(52) Jeanne Dit Fouque, K.; Hegemann, J. D.; Zirah, S.; Rebuffat, S.; Lescop, E.; Fernandez-Lima, F. Evidence of *Cis/Trans*-Isomerization at Pro7/Pro16 in the Lasso Peptide Microcin J25. *J. Am. Soc. Mass Spectrom.* **2019**, *30* (6), 1038−1045.

(53) Jeanne Dit Fouque, K.; Lavanant, H.; Zirah, S.; Hegemann, J. D.; Fage, C. D.; Marahiel, M. A.; Rebuffat, S.; Afonso, C. General Rules of Fragmentation Evidencing Lasso Structures in CID and ETD. *Analyst* **2018**, *143* (5), 1157−1170.

(54) Güntert, P.; Buchner, L. Combined Automated NOE Assignment and Structure Calculation with CYANA. *J. Biomol. NMR* **2015**, *62* (4), 453−471.

(55) Bayro, M. J.; Mukhopadhyay, J.; Swapna, G. V. T.; Huang, J. Y.; Ma, L.-C.; Sineva, E.; Dawson, P. E.; Montelione, G. T.; Ebright, R. H. Structure of Antibacterial Peptide Microcin J25: A 21-Residue Lariat Protoknot. *J. Am. Chem. Soc.* **2003**, *125* (41), 12382−12383.

(56) Rosengren, K. J.; Clark, R. J.; Daly, N. L.; Göransson, U.; Jones, A.; Craik, D. J. Microcin J25 Has a Threaded Sidechain-to-Backbone Ring Structure and Not a Head-to-Tail Cyclized Backbone. *J. Am. Chem. Soc.* **2003**, *125* (41), 12464−12474.

(57) Hegemann, J. D.; Zimmermann, M.; Xie, X.; Marahiel, M. A. Caulosegnins I−III: A Highly Diverse Group of Lasso Peptides Derived from a Single Biosynthetic Gene Cluster. *J. Am. Chem. Soc.* **2013**, *135* (1), 210−222.

(58) Hegemann, J. D.; Zimmermann, M.; Zhu, S.; Steuber, H.; Harms, K.; Xie, X.; Marahiel, M. A. Xanthomonins I-III: A New Class of Lasso Peptides with a Seven-Residue Macrolactam Ring. *Angew. Chem. Int. Edit.* **2014**, *53* (8), 2230−2234.

(59) Son, S.; Jang, M.; Lee, B.; Hong, Y.-S.; Ko, S.-K.; Jang, J.-H.; Ahn, J. S. Ulleungdin, a Lasso Peptide with Cancer Cell Migration Inhibitory Activity Discovered by the Genome Mining Approach. *J. Nat. Prod.* **2018**, *81* (10), 2205−2211.

(60) Tan, S.; Moore, G.; Nodwell, J. Put a Bow on It: Knotted Antibiotics Take Center Stage. *Antibiotics (Basel)* **2019**, *8* (3), 117.

(61) Brady, C.; Cleenwerck, I.; Venter, S.; Coutinho, T.; de Vos, P. Taxonomic Evaluation of the Genus *Enterobacter* Based on Multilocus Sequence Analysis (MLSA): Proposal to Reclassify *E. nimipressuralis* and *E. amnigenus* into *Lelliottia* gen. nov. as *Lelliottia nimipressuralis* comb. nov. and *Lelliottia amnigena* comb. nov., respectively, *E. gergoviae* and *E. pyrinus* into *Pluralibacter* gen. nov. as *Pluralibacter gergoviae* comb. nov. and *Pluralibacter pyrinus* comb. nov., Respectively, *E. cowanii, E. radicincitans, E. oryzae* and *E. arachidis* into *Kosakonia* gen. nov. as *Kosakonia cowanii* comb. nov., *Kosakonia radicincitans* comb. nov., *Kosakonia oryzae* comb. nov. and *Kosakonia arachidis* comb. nov., Respectively, and *E. turicensis, E. helveticus* and *E. pulveris* into *Cronobacter* as *Cronobacter zurichensis* nom. nov., *Cronobacter helveticus* comb. nov. and *Cronobacter pulveris* comb. nov., respectively, and Emended Description of the Genera *Enterobacter* and *Cronobacter*. *Syst. Appl. Microbiol.* **2013**, *36* (5), 309−319.

(62) Zhu, B.; Lou, M.-M.; Xie, G.-L.; Wang, G.-F.; Zhou, Q.; Wang, F.; Fang, Y.; Su, T.; Li, B.; Duan, Y.-P. *Enterobacter mori* sp. nov., associated with bacterial wilt on *Morus alba* L. *Int. J. Syst. Evol. Micr.* **2011**, *61* (11), 2769−2774.

(63) Koth, K.; Boniface, J.; Chance, E. A.; Hanes, M. C. *Enterobacter asburiae* and *Aeromonas hydrophila*: Soft Tissue Infection Requiring Debridement. *Orthopedics* **2012**, *35* (6), No. e996-9.

(64) Westerfeld, C.; Papaliodis, G. N.; Behlau, I.; Durand, M. L.; Sobrin, L. *Enterobacter amnigenus* Endophthalmitis. *Retin. Cases Brief Rep.* **2009**, *3* (4), 409−411.

(65) Xue, Y.; Hu, M.; Chen, S.; Hu, A.; Li, S.; Han, H.; Lu, G.; Zeng, L.; Zhou, J. *Enterobacter asburiae* and *Pantoea ananatis* Causing Rice Bacterial Blight in China. *Plant Dis.* **2021**, *105* (8), 2078−2088.

(66) Ren, Y.; Ren, Y.; Zhou, Z.; Guo, X.; Li, Y.; Feng, L.; Wang, L. Complete Genome Sequence of *Enterobacter cloacae* subsp. *cloacae* Type Strain ATCC 13047. *J. Bacteriol.* **2010**, *192* (9), 2463−2464.

(67) Salamzade, R.; Manson, A. L.; Walker, B. J.; Brennan-Krohn, T.; Worby, C. J.; Ma, P.; He, L. L.; Shea, T. P.; Qu, J.; Chapman, S. B.; Howe, W.; Young, S. K.; Wurster, J. I.; Delaney, M. L.; Kanjilal, S.; Onderdonk, A. B.; Bittencourt, C. E.; Gussin, G. M.; Kim, D.; Peterson, E. M.; Ferraro, M. J.; Hooper, D. C.; Shenoy, E. S.; Cuomo, C. A.; Cosimi, L. A.; Huang, S. S.; Kirby, J. E.; Pierce, V. M.; Bhattacharyya, R. P.; Earl, A. M. Inter-Species Geographic Signatures for Tracing Horizontal Gene Transfer and Long-Term Persistence of Carbapenem Resistance. *Genome Med.* **2022**, *14* (1), 37.

(68) Do, T.; Thokkadam, A.; Leach, R.; Link, A. J. Phenotype-Guided Comparative Genomics Identifies the Complete Transport Pathway of the Antimicrobial Lasso Peptide Ubonodin in *Burkholderia*. *ACS Chem. Biol.* **2022**, *17*, 2332.

(69) DiCaprio, A. J.; Firouzbakht, A.; Hudson, G. A.; Mitchell, D. A. Enzymatic Reconstitution and Biosynthetic Investigation of the Lasso Peptide Fusilassin. *J. Am. Chem. Soc.* **2019**, *141* (1), 290−297.

(70) Pavlova, O.; Mukhopadhyay, J.; Sineva, E.; Ebright, R. H.; Severinov, K. Systematic Structure-Activity Analysis of Microcin J25. *J. Biol. Chem.* **2008**, *283* (37), 25589−25595.

(71) Knappe, T. A.; Linne, U.; Robbel, L.; Marahiel, M. A. Insights into the Biosynthesis and Stability of the Lasso Peptide Capistruin. *Chem. Biol.* **2009**, *16* (12), 1290−1298.

(72) Liu, T.; Ma, X.; Yu, J.; Yang, W.; Wang, G.; Wang, Z.; Ge, Y.; Song, J.; Han, H.; Zhang, W.; Yang, D.; Liu, X.; Ma, M. Rational Generation of Lasso Peptides Based on Biosynthetic Gene Mutations and Site-Selective Chemical Modifications. *Chem. Sci.* **2021**, *12* (37), 12353−12364.

(73) Zimmermann, M.; Hegemann, J. D.; Xie, X.; Marahiel, M. A. The Astexin-1 Lasso Peptides: Biosynthesis, Stability, and Structural Studies. *Chem. Biol.* **2013**, *20* (4), 558−569.

(74) Hegemann, J. D.; Fage, C. D.; Zhu, S.; Harms, K.; Di Leva, F. S.; Novellino, E.; Marinelli, L.; Marahiel, M. A. The Ring Residue Proline 8 Is Crucial for the Thermal Stability of the Lasso Peptide Caulosegnin II. *Mol. Biosyst.* **2016**, *12* (4), 1106−1109.

(75) Schröder, H. V.; Zhang, Y.; Link, A. J. Dynamic Covalent Self-Assembly of Mechanically Interlocked Molecules Solely Made from Peptides. *Nat. Chem.* **2021**, *13* (9), 850−857.

⧉ Recommended by ACS

Mammalian Commensal *Streptococci* Utilize a Rare Family of Class VI Lanthipeptide Synthetases to Synthesize Miniature Lanthipeptide-type Ribosomal Peptide Natural...

Yile He, Yigang Tong, *et al.*

DECEMBER 28, 2022
BIOCHEMISTRY   READ ☑

Unusual Class I Lanthipeptides from the Marine Bacteria *Thalassomonas viridans*

Ross Vermeulen, Marla Trindade, *et al.*

NOVEMBER 02, 2022
ACS SYNTHETIC BIOLOGY   READ ☑

Measurement of Small Molecule Accumulation into Diderm Bacteria

George M. Ongwae, Marcos M. Pires, *et al.*

DECEMBER 18, 2022
ACS INFECTIOUS DISEASES   READ ☑

Engineering of Specific Single-Module Nonribosomal Peptide Synthetases of the RXP Type for the Production of Defined Peptides

Xiaofeng Cai, Helge B. Bode, *et al.*

DECEMBER 19, 2022
ACS SYNTHETIC BIOLOGY   READ ☑

Get More Suggestions >